Volume : 2 | Issue : 9 | Sept 2013 ISSN - 2250-1991

Research Paper Engineering

Effect of Plate Materials and Ambient Conditions on The Design of Flate Plate Solar Collector

* Dr. Qusay A. Jawad *** Dheya N. Abdulamer

* Lecturer, Energy and Renewable Energies Technology Center, University of Technology, Baghdad, Iraq

** Assistant lecturer, Energy and Renewable Energies Technology Center, University of Technology, Baghdad, Iraq

ABSTRACT

Flat plate solar collector radiation from the sun and transfer the received energy to a fluid which passing through pipes or channels which are integrating with the collector absorber plate that has a physical properties characterized by high absorptive solar radiation and low emission called the absorption surface, typically a metal plate, usually copper, aluminum alloy and steel materials with tubing of copper in thermal contact with the plates. In this paper simple and efficient thermal system has been designed to utilize the available sun light by simple design of flat plate solar collector under different conditions which includes different climatic conditions and different types of plate materials. For each case of above it was found outlet fluid temperature, instantaneous efficiency and modifier angle factor.

Keywords : Flat plate solar collector; Solar collector; thermal efficiency of collector

1. Introduction

In the recent years solar energy has been strongly promoted as an active energy source. One of the simplest and most direct applications of this energy is the conversion of solar radiation into heat. Hence way that the domestic sector can lessen its impact on the environment is by the installation of solar flat plate collectors for heating water. Although it should be said that some of these collectors have been in service for the last 40-50 years without any real significant changes in their design and operational principles. A typical flat-plate collector consists of an absorber in an insulated box together with transparent cover sheets (glazing) [1]. The absorber is usually made of a metal sheet of high thermal conductivity, such as copper or aluminum, with integrated or attached tubes Fig. 1. Its surface is coated with a special selective material to maximize radiant energy absorption while minimizing radiant energy emission. The insulated box reduces heat losses from the back and sides of the collector [2 - 3]. The flow distribution through the finned tubes of a collector clearly affects the operational efficiency of the collector system. Therefore, the more uniform the flow through the tubes, then the higher efficiency of the collector, and vice versa [4 - 5]. The flow distribution can be evaluated by temperature measurements at various points of the collector [6]. The energy loss through the top of solar collector is the result of convection and radiation between the parallel plates. The loss per unit area through the top is equal to the heat transfer from the absorber plate to the cover. This process of losing energy illustrated in fig.2.

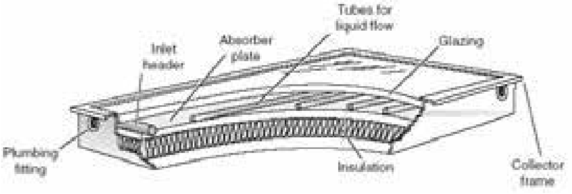

Figure 1. Flat plate solar collector [3]

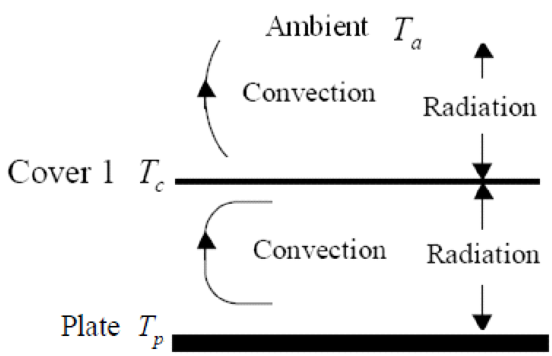

Figure 2. Heat transfer mechanisms through a collector with a single cover [6]

There are another source of heat losses which are the back and edge heat losses of the collector where the energy loss through the back of the collector is the outcome of the conduction through the back insulation and the convection and radiation heat transfer from the back of the collector to surroundings. The magnitudes of the thermal resistance of convection and radiation heat transfer are much smaller than that of conduction, and therefore it can be assumed that all the thermal resistance from the back is due to the insulation [7]. To guarantee that the collector can withstand high thermal loads, the highest temperature in the collector should be less than the melting point of the parts that is assembled from. Stagnation temperatures are the highest temperatures of the covers and absorber plate that can be obtained from the collector. They take place when the collector is not working, i.e. when the working fluid does not circulate. In this case, the useful gain from the collector is zero [8]. The collector can reach temperatures up to 200°C when no liquid flows through it and therefore all the materials used must be able to resist such heat. The absorber is usually made of metallic materials such as copper, steel or aluminum. The collector housing can be made of plastic, metal or wood, and the glass front cover must be sealed so that heat does not escape, and the collector itself is protected from dirt, insects or humidity. The absorber plate which covers the full aperture area of the collector must perform three functions: absorb the maximum possible amount of solar irradiance, transfer this heat into the working fluid at a minimum temperature difference and lose a minimum amount of heat back to the surroundings. Since the temperature of the absorber surface is above ambient temperature, the surface re-radiates some of the heat it has absorbed back to the surroundings. This loss mechanism is a function of the emittance of the surface for low-temperature, long-wavelength radiation. Many coatings that enhance the absorption of sunlight (short-wavelength radiation) also enhance the long wavelength radiation loss from the surface. A good coating will produce an absorber surface that is a good absorber of short-wavelength solar irradiance but a poor emitter of long-wavelength radiant energy. Normally the absorber is covered with one or more transparent cover sheets to reduce convective heat loss. However convective loss is not completely eliminated because a convective current exists between the absorber and the cover sheet, so transferring heat from the absorber to the cover sheet. External convection then produces a net heat loss from the absorber as it cools the cover sheet.

2. Theoretical background

Under steady conditions, the useful heat delivered by solar collector is equal to the energy absorbed in the metal surface minus the heat losses from the surface directly and indirectly to the surroundings. This principle can be stated in the relationship:

$$Q_u = A_c\,[HR\,(\tau.\alpha)_e - U_L\,(t_p - t_a)] \qquad (1)$$

Where Q_u is the useful energy delivered by collector, [Watts] or [cal hr^{-1}]. A_c is the collector area, [m^2]. *HR* is the solar energy received on the upper surface of slopping collector, [W m^{-2}] or [kcal hr^{-1} m^{-2}] . H is the rate of incident beam or diffuse radiation on a unit area of surface of any orientation. *R* is the factor to convert beam or diffuse radiation to that on the plane of collector. τ is the fraction of incoming solar radiation that reaches the absorbing surface, transmissivity (dimensionless). α is the fraction of solar energy reaching the surface that is absorbed, absorptivity (dimensionless). $(\tau . \alpha)_e$ is the effective transmittance absorptance product of cover system for beam and diffuse radiation. U_L is the overall heat loss coefficient. t_p is the average temperature of the upper surface of the absorber, [°C] and t_a is the atmospheric temperature, [°C]. The factors in eq. 1 depend on the collector design, operating conditions, solar energy and atmospheric temperature. The energy balance equation on the whole collector can written as:

$$A_c\,[HR\,(\tau.\alpha)_e + HR\,(\tau-\alpha)_d\,] = Q_u + Q_l + Q_e \qquad (2)$$

Where Q_u = rate of useful heat transfer to a working fluid in the solar heat exchanger. Q_l = rate of energy losses from the collector to the surroundings. Q_e = rate of energy storage in the collector. Collector efficiency r_c is the collector performance and is defined as the ratio of useful gain over any time period to the incident solar energy over the same time period.

$$r_c = \frac{\int Q_u\, d_T}{\int HR\, d_T} \qquad (3)$$

$$\frac{d^2T}{dx^2} = \frac{U_L}{K\delta}\left(T - T_a - \frac{S}{U_L}\right) \qquad (4)$$

The equation .4 becomes

The general solution is :

$$x = C_1 \sinh m + C_2 \cosh m \qquad (6)$$

The constants C_1 and C_2 are found by substituting boundary conditions. The eq. 6 becomes:

$$\frac{T - T_a - S/U_L}{T_b - T_a - S/U_L} = \frac{\cosh m}{\cosh m\,(\frac{W-D}{2})} \qquad (7)$$

The energy conducted to the region of the tube per unit length in the flow direction is

$$q^1{}_{finbase} = \frac{K\,\delta\, m}{U_L}[S - UL\,(Tb - Ta)]\tanh\left(\frac{W-D}{2}\right)m \qquad (8)$$

The equation. 8 accounts for the energy collected to only one side of a tube. The useful gain of the collector also includes the energy collected above the tube region. The energy gain for the region:

$$q_{tube} = D[S - U_L\,(T_b - T_a)] \qquad (9)$$

Hence, the total energy gain of the collector tubes per unit length in the flow direction may be expressed as:

$$q_u = q_{finbase} + qt_{ube\,section} \qquad (10)$$

Ultimately, the useful gain from the eq. 8 must be transferred into the fluid. The resistance to heat flow to the tube from the plant due to the wall thickness of the tube. Hence

$$q_u = \frac{Tb - Tf}{\frac{1}{C_b} + \frac{1}{\pi D_i h_{fi}} + \frac{1}{C_w}} \qquad (11)$$

Where C_b = the conductance of the bond. C_w = the conductance of the tube wall and h_{fi} = the local film heat transfer coefficient. The bond conductance is given as :

$$C_b = \frac{K_b\, b}{y} \qquad (12)$$

Where K_b = bond conductivity, *b* = bond length and *y* = bond average thickness. The useful energy gain of the fluid can then be expressed in terms of the known dimensions, the physical parameters and the local fluid temperature by solving the eq.11 for T_b and substituting to obtain q_u from eq.10.

$$q_u = WF^1\,[S - U_L\,(T_f - T_a)] \qquad (13)$$

Where,

$$F^1 = \frac{1/U_L}{W\left[\frac{1}{UL[D+(W-D)F]} + \frac{1}{C_b} + \frac{1}{C_w} + \frac{1}{\pi D_i h_{fi}}\right]} \qquad (14)$$

For temperature distribution in the flow direction, consider the energy balance on the fluid element flowing through a pipe which is receiving a uniform heat flux q_u so that :

$$m^\bullet C_p T_f \big|y - m^\bullet C_p T_f \big|_{y+dy} + \Delta y_1\, q_u = 0 \qquad (15)$$

0 Driving through by Δ*y* and finding the limit Δ*y*

and substituting in Eq.15.

$$m^\bullet C_p \frac{dT_f}{dy} - WF^1[S - U_L\,(T_f - T_a)] = 0 \qquad (16)$$

If the assumption is made that F^1 and U_L are constant (and independent of *y*) , than the solution of the differential equation for the temperature at any position (if subject to the condition that inlet fluid temperature is T_{fi}) is :

$$\frac{T_f - T_a - S/U_L}{T_f i - T_a - S/U_L} = e^{-(U_L\ WF^1\ y/m^\bullet C_p)} \qquad (17)$$

If the collector has length *L* in the flow direction, then the outlet fluid temperature T_{f° is found by substituting *L* for *y* in the eq. 17.

$$T_{f\circ} = T_a + \left(\frac{S}{U_L}\right) - \left[\frac{S}{U_L} - (T_f - T_a)\right)^{e - U_L F^1 A_\circ / m^\bullet C_p} \quad (18)$$

Where : $A_c = WL$, the area of collector. The total useful energy collection rate Q_u may be expressed as :

$$Q_u = m^\bullet \; C_p \; (T_f - T_a) \quad (19)$$

Substituting for $T_{f\circ}$ already derived, gives:

$$Q_u = A_c \, F_R [\, S - U_L \, (T_f - T_a) \quad (20)$$

Where
$$F_R = \frac{G C_p}{U_L} [1 - e^{-u_L F^1 l G C_p}) \quad (21)$$

F_R has been termed as the heat removal factor of the collector.

3. Modeling and Design

The following tables represent steps of the main considerations that tack into account during modeling flat plate solar collector using *EES* soft program.

Table 1. Test conditions

State	G_T [W m^{-2}]	G_d / G_T [%]	θ [deg]	β [deg]	T amb [ºC]	V wind [m s^{-1}]	R [%]
A	1000	2	30	30	30	2.5	25
B	1000	2	30	30	40	2.5	25
C	1000	2	30	30	50	2.5	25

Efficiency curves based on temperature difference : T_{av} - T_a

Table 2. Dimensions of collector

Overall dimensions			Absorber dimensions	
L [m]	W [m]	t [m]	L_p [m]	W_p [m]
2.91	1.221	0.079	2.4	1.137

L = Length, *W*= Width , *t* = Thickness (m), L_p = Length, W_p = Width

Table 3. Properties of glass Cover

	Properties of Cover 1				Properties of Cover 2			
	Solar Spectrum		Long-wave		Solar Spectrum		Long-wave	
Number of Cover	n	$_{c,s}T$	$_c\varepsilon$	$_{c,IR}T$	n	$_{c,s}T$	$_c\varepsilon$	$_{c,IR}T$
2	1.526	0.891	0.88	0	1.526	0.891	0.88	0

d_{cp} = Cover- plate air spacing = 1.8 [cm], $d_{c1,c2}$ = Cover 1- cover 2 air spacing = 0.5 [cm]

Table 4. Properties of Plate material

Plate Material	K_{pl} [w m^{-1}.K^{-1}]	t_p[cm]	d_n	ε_{pl}
Cu	380	0.02	0.88	0.15
Al – alloy 2024 T6	177	0.02	0.88	0.15
Plain carbon steel	60.5	0.02	0.88	0.15

K_{pl} = user defined conductivity, t_p = Thickness, d_n = Absorptance, ε_{pl} = Emittance

Table 5. Number and dimension of tube

N_t	d_i [cm]	$d_\circ$ [cm]
10	1.6	1.8

N_t = Number of Tubes, d_i = Inner diameter, $d_\circ$ = Outer diameter

Table 6. Properties of Fluid

Material	$V^\cdot$ [L/min]	P_{in} [KPa]	K_b [w/m.K]
Water	1	200	400

$V^\cdot$ = Volumetric flow rate, P_{in} = Inlet pressure, K_b = Plate tube bond conductance

Table 7. Edge and back insulation

Property	Edge insulation	Back insulation
Conductivity [W m^{-1} . K^{-1}]	0.04	0.04

4. Results and discussion:

The instantaneous efficiency of flat plate solar collector have different type of plate materials and exposure into various temperature have great effects. Fig .3, show the instantaneous efficiency of flat plate solar collector has copper plate and exposure into 30 °C start from 0.6 and decrease with increased of *∆T/GT* then reach in to minimum value 0.35. Small match of the instantaneous efficiency between design and experimental has been shown. A little divergence of the instantaneous efficiency between design and experimental has been shown in solar collector has aluminum alloy plate and exposure into same temperature as mentioned in fig. 6. In this case, the instantaneous efficiency start from 0.575, while the instantaneous efficiency solar collector has carbon steel plate and exposure into same temperature is 0.512. In this context, large divergence of instantaneous efficiency between design and experimental as shown in fig. 9. In contrast, same behavior above of the instantaneous efficiency between design and experimental for solar collector have copper, aluminum alloy and carbon steel plate and exposure into 40 °C and 50 °C respectively. Just values of the instantaneous efficiency of solar collector changes from case of exposure into 30 °C, these values is obviously shown in figures 12, 15, 18, 21, 24 and 27 respectively.

Temperature distribution of flat plate solar collector has copper plate and exposure into 30 °C is shown in fig. 5, where 94.27 °C is the temperature of first cover glass, 59.27 °C is the temperature of second cover glass and 169.7 °C is the temperature of copper plate. Same temperature distribution is shown figures 8 and 11 for solar collector has aluminum alloy and plain carbon steel plate respectively, and exposure into 30 °C. As the solar collector exposure into high temperature 40 °C, temperature distribution of the collector for first cover glass, second cover glass are 102.6 °C, 69.25 °C respectively and temperature of copper, aluminum alloy and carbon steel plate 177.8 °C as shown in figures 14, 17 and 20. When incident temperature increased in to 50 °C, temperature developed at solar collector are 111.6 °C, 79.9 °C, for first cover glass, second cover glass. Figures 23, 26 and 29 show 186.3 °C is the maximum temperature generated on the copper, aluminum alloy and carbon steel plate.

5. Conclusions

The instantaneous efficiency of flat plate solar collector greatly affected by incident temperature and type of plate materials. However, the values of the instantaneous efficiency extend from 0.6 to 0.25 with change of *∆T/GT* for all various parameters of exposure temperature and type of plate materials. For all exposure temperature, closely match of the instantaneous efficiency between design and experimental clearly found in the case of copper plate, while a little and large divergence occurred in the cases of aluminum alloy and carbon steel plate respectively. In this context, at different exposure temperature, same temperatures are developed in plate for all type of materials.

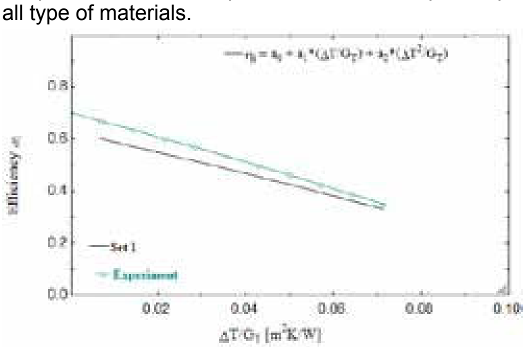

Figure 3. Instantaneous Efficiency of collector for copper plate at 30 °C

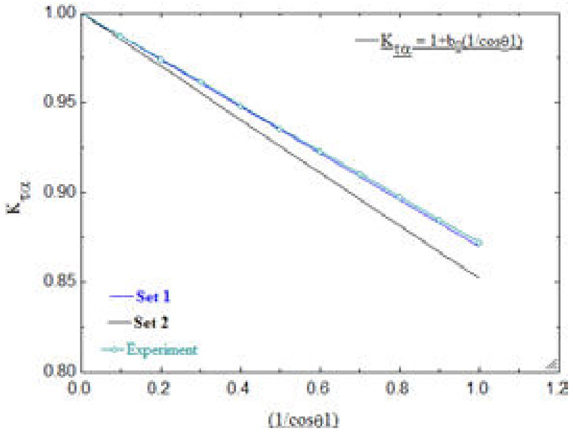

Figure 4. Incident Ingle Modifier for copper plate at 30 °C

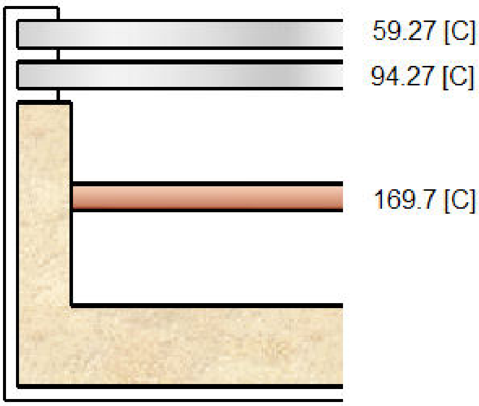

Figure 5. Temperature distribution for copper plate at 30 °C

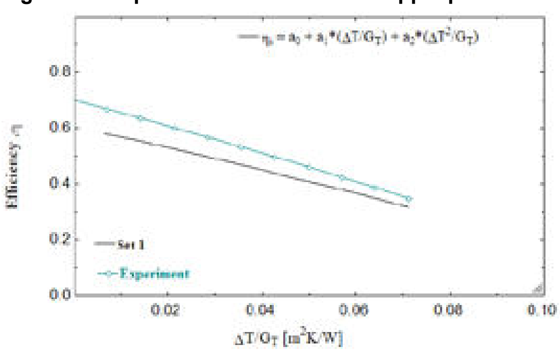

Figure 6. Instantaneous Efficiency of collector for Aluminum alloy plate at 30 °C

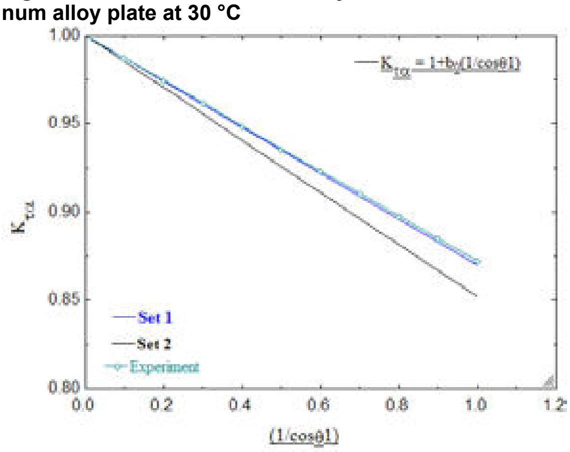

Figure 7. Incident Ingle Modifier for Aluminum alloy plate at 30 °C

Figure 8. Temperature distribution for Aluminum alloy plate at 30 °C

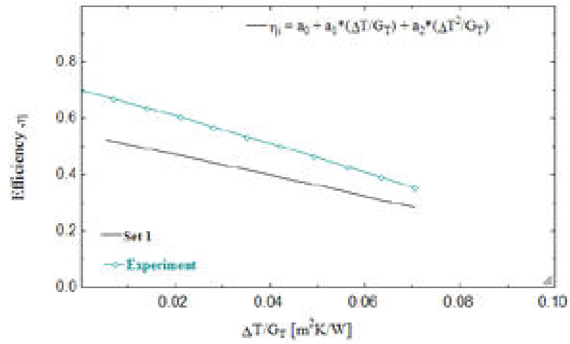

Figure 9. Instantaneous Efficiency of collector for Plain carbon steel plate at 30 °C

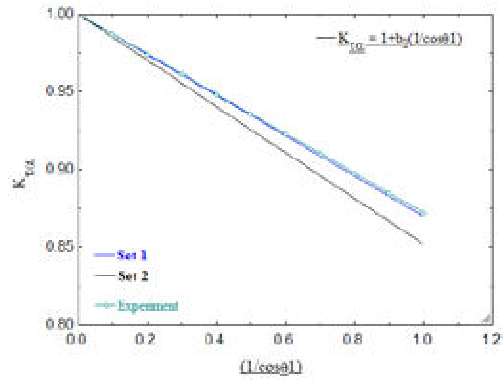

Figure 10. Incident Ingle Modifier for Plain carbon steel plate at 30 °C

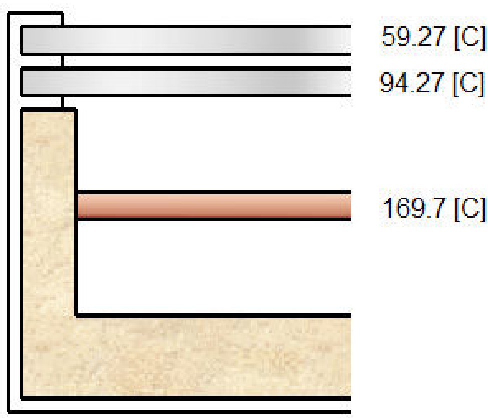

Figure 11. Temperature distribution for Plain carbon steel plate at 30 °C

ISSN - 2250-1991

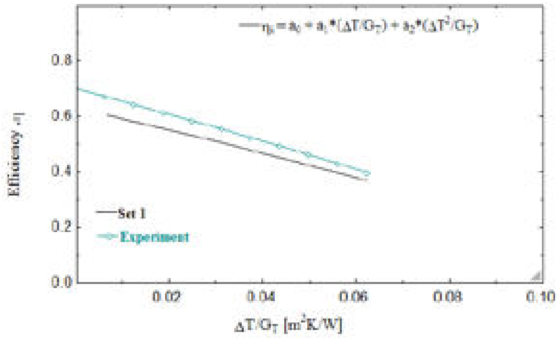

Figure 12. Instantaneous Efficiency of collector for Copper plate at 40 °C

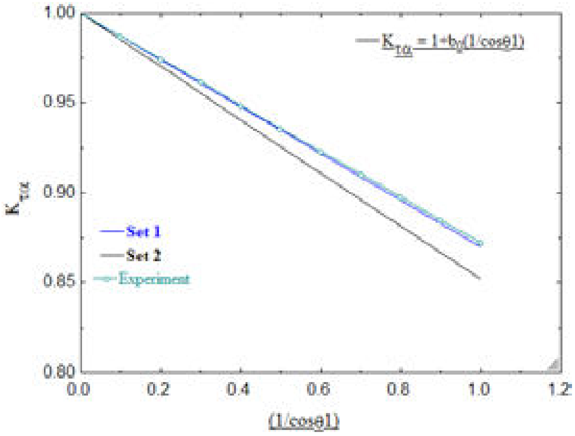

Figure 13. Incident Ingle Modifier for Copper plate at 40 °C

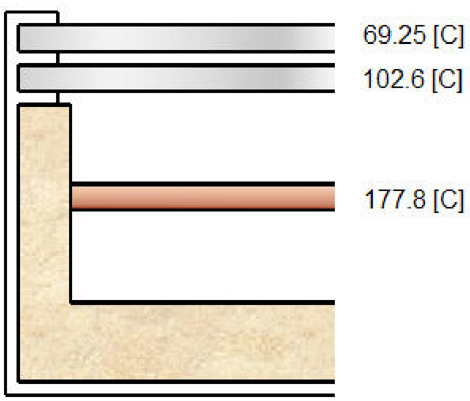

Figure 14. Temperature distribution for Copper plate at 40 °C

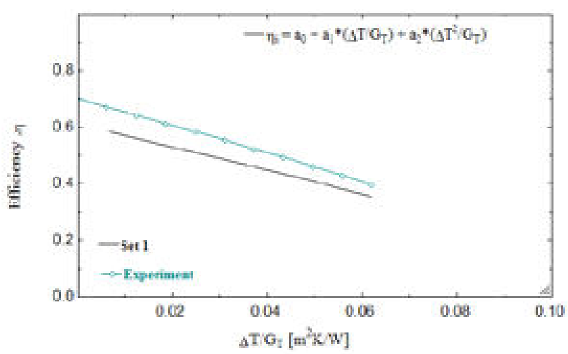

Figure 15. Instantaneous Efficiency of collector for Aluminum alloy plate at 40 °C

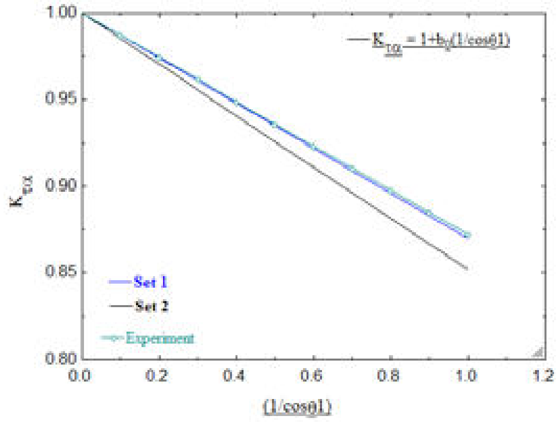

Figure 16. Incident Ingle Modifier for Aluminum alloy plate at 40 °C

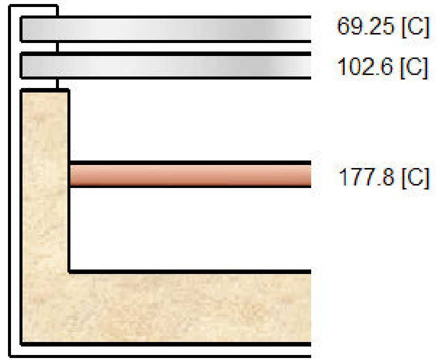

Figure 17. Temperature distribution for Aluminum alloy plate at 40 °C

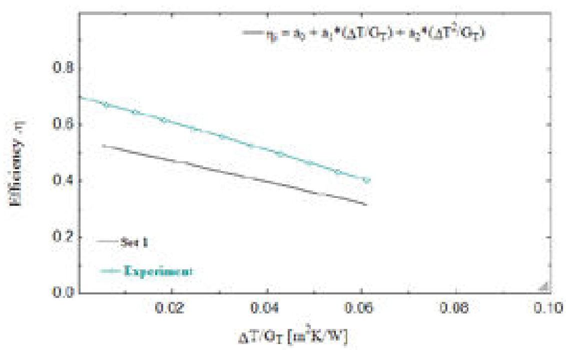

Figure 18. Instantaneous Efficiency of collector for Plain carbon steel plate at 40 °C

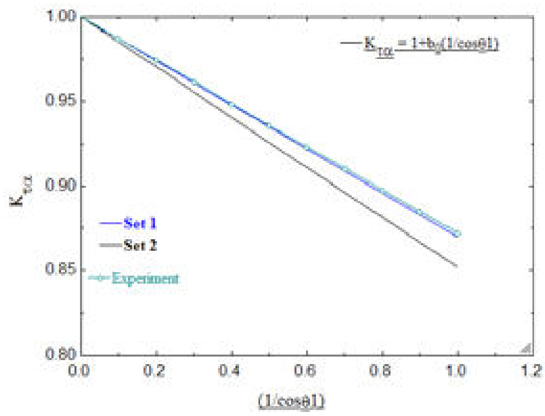

Figure 19. Incident Ingle Modifier for Plain carbon steel plate at 40 °C

 ISSN - 2250-1991

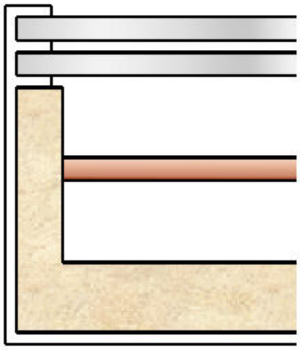

Figure 20. Temperature distribution for Plain carbon steel plate at 40 °C

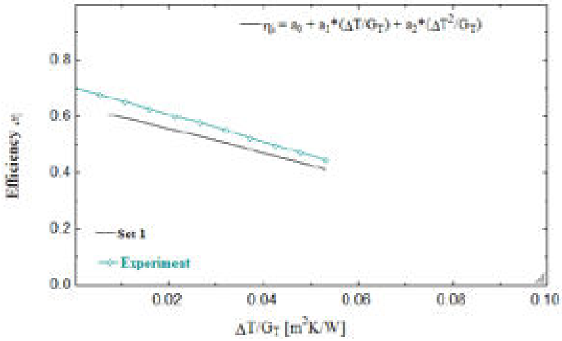

Figure 21. Instantaneous Efficiency of collector for Copper plate at 50 °C

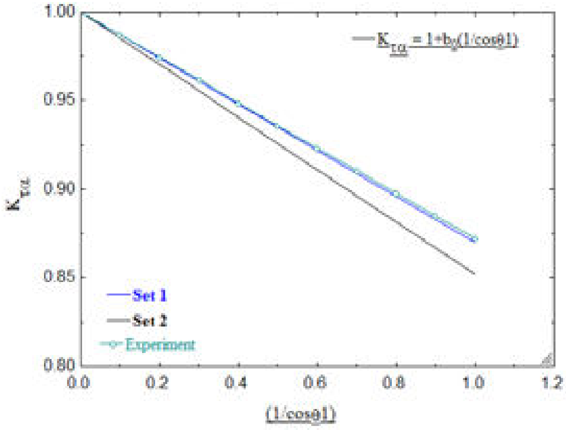

Figure 22. Incident Ingle Modifier for Copper plate at 50 °C

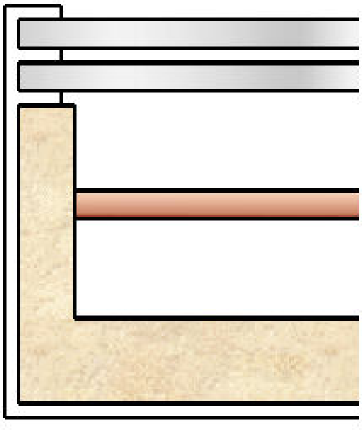

Figure 23. Temperature distribution for Copper plate at 50 °C

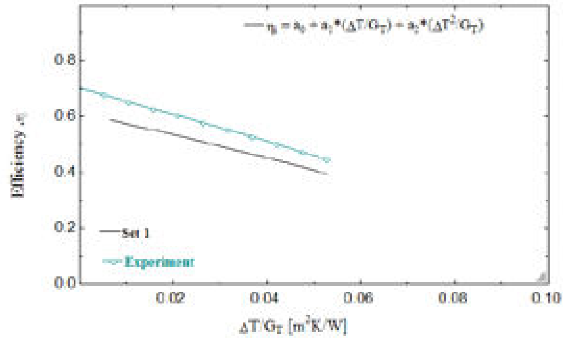

Figure 24. Instantaneous Efficiency of collector for Aluminum alloy plate at 50 °C

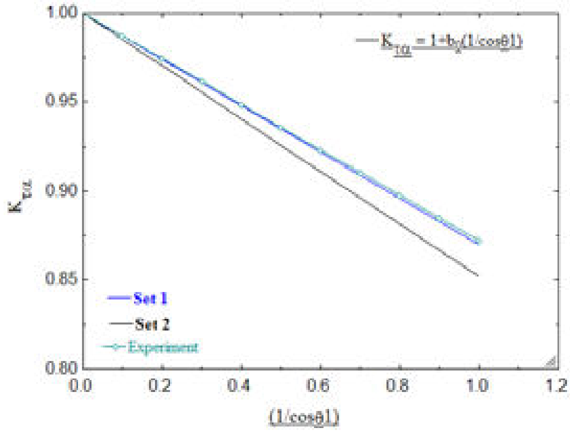

Figure 25. Incident Ingle Modifier for Aluminum alloy plate at 50 °C

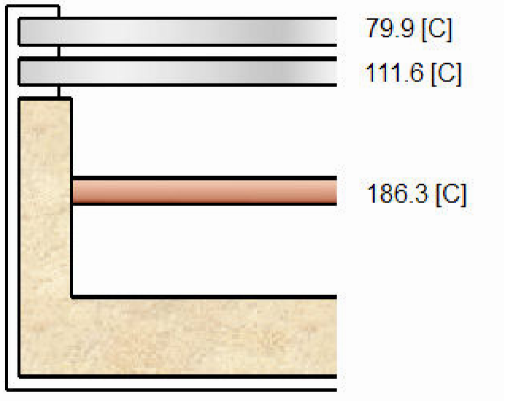

Figure 26. Temperature distribution for Aluminum alloy plate at 50 °C

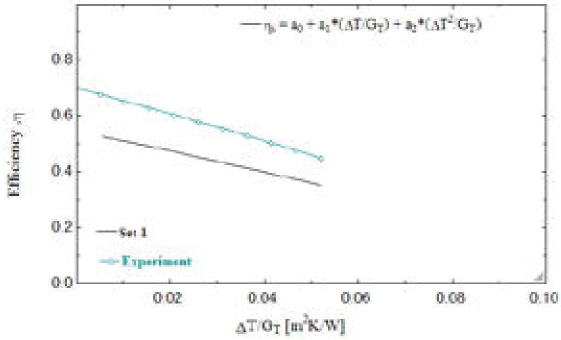

Figure 27. Instantaneous Efficiency of collector for Plain carbon steel plate at 50 °C

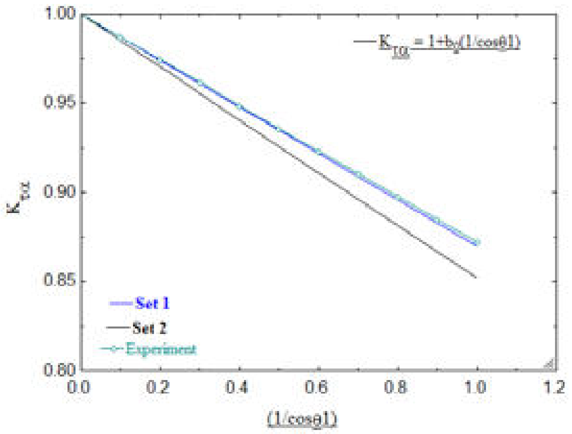

Figure 28. Incident Ingle Modifier for Plain carbon steel plate at 50 °C

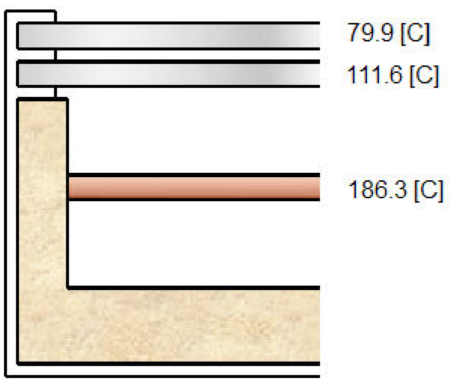

Figure 29. Temperature distribution for Plain carbon steel plate at 50 °C

Nomenclature

r_c - Collector efficiency.

q_{tube} - Energy collected above the tube region, Watts.

q_u - Total energy gain of the collector, Watts.

C_b - Bond conductance

T_{fi} - Inlet fluid temperature, °C.

T_{f° - Outlet fluid temperature, °C.

G_T - Incident Solar Radiation, W/m^2.

θ -Incident Angle of Beam Radiation, deg.

β - Collector slope, deg.

T_{amb} -Ambient Temperature, °C.

V_{wind} - Wind speed, m/s.

F^1 -Collector efficiency factor.

G_d/G_T -Diffuse Radiation proportion.

R - Relative Humidity.

REFERENCES

[1] ***, U.S. Department of Energy - Energy Efficiency and Renewable Energy Solar Energy Technologies Program, http://www.eere.energy.gov/solar/ | [2] Duffie, J. A. and W. A. Beckman, Solar Engineering of Thermal Processes, John Wiley and Sons Inc, New York, USA, 1991 | 3.Charles Smith, History of Solar Energy Revisiting, Past Solar Power Technology Review,1995. | [4] G.F Jones and N. Lior, Flow distribution in manifold solar collectors with negligible buoyancy effects. Solar Energy. , 52 (1994), P.P. 289–300 | [5] ***, Solar Thermal Tech, Sandia National Labs, http://www. solstice.crest.org/renewable | [6] V. Weitbrecht, D. Lehmann and A. Richter, Flow distribution in solar collectors with laminar flow conditions, Solar Energy . , 73 (2002), P.P. 433-441 | [7] V. Kienzlen, J.M. Gordon and J.F Kreider, The reverse flat plate collector: A stationary,non evacuated, low-technology, medium-temperature solar collector, Solar Energy Engineering. , 110 (1988), P.P. 23-30 | [8] IORDANOU, GRIGORIOS, Flat-Plate Solar Collectors for Water Heating with Improved Heat Transfer for Application in Climatic Conditions of the Mediterranean Region, Msc. thesis, Durham university , 2009. |